ANALYTICAL STUDY OF THE PERFORMANCE SURFACE OF BLIND EQUALIZER IN A COSINE MODULATED MULTICARRIER COMMUNICATION SYSTEM

Lekun Lin and Behrouz Farhang-Boroujeny

Department of Electrical and Computer Engineering
University of Utah
Salt Lake City, UT84112
e-mails: llin@eng.utah.edu and farhang@ece.utah.edu.

ABSTRACT

A recent development in the literature has proposed a cosine modulated filter bank-based multicarrier modulation technique with blind equalization capability. However, convergence studies of the proposed blind equalizer has been carried out through computer simulations only. In this paper, we present a thorough study of the blind equalizer by analyzing its associated cost function and show that it has two global minimum and two saddle points.

1. INTRODUCTION

Multicarrier modulation (MCM) has attracted considerable attention in recent years as a practical and viable technology for high-speed data transmission over spectrally shaped noisy channels [1, 3]. The discrete multitone/orthogonal frequency division multiplexing (DMT/OFDM) has been recognized as the most cost effective realization of multicarrier transceivers in both wired [2], and wireless [3] channels.

Cosine modulated filter banks (CMFB) working at maximally decimated rate, on the other hand, are well understood and widely used for signal compression [5]. Moreover, the use of CMFB to multicarrier data transmission over digital subscriber lines (DSL) has been widely addressed in the literature, under the common terminology of discrete wavelet multitone (DWMT) [4].

The major problem with DWMT is the need for a set of special equalizers, one per subchannel. These equalizers that are referred to as linear combiners [4] are two dimensional equalizers that span across time and frequency. Each linear combiner usually needs at least 21 taps (7 taps along time and 3 taps along frequency axis) to perform satisfactorily. This relatively large number of coefficients per linear combiner has the disadvantages of high computational complexity and slow convergence. These difficulties have made DWMT non-attractive to industry, even though it offers higher bandwidth efficiency (because of absence of cyclic extensions) and more immunity to narrowband interference.

A revisit of DWMT has been made recently [7, 8]. This new study has shown that a modification to the receiver structure in DWMT allows deployment of equalizers that require only two taps per subchannel. Moreover, a blind algorithm that can be used for adaptation of such equalizers has been proposed. Extensive computer simulations presented in [7, 8] show that the proposed blind equalizer converges to one of its global minima if initialized properly. In another study [9], we derived analytical expression for the performance function of the blind equalizer, found it has four critical points, from which two are global minima. However, the nature of the other critical points could be only studied graphically. In this paper, we complete our study by proving that the latter are saddle points.

2. SYSTEM MODEL

The multicarrier modulation system that has been proposed in [7, 8] is based on the assumption that the number of subchannels is sufficiently large so that each subchannel can be approximated by a flat gain. With this assumption, each subchannel of the system may be modeled as in Fig. 1. The input to the subchannel is a complex variable whose real part is the transmitted PAM signal, $s(n)$, and its imaginary part, $u(n)$, arises from intersymbol interference (ISI) from the same subchannel and interchannel interference (ICI) from the adjacent subchannels. Since $u(n)$ is a combination of a large number of random variables (ISI and ICI components), it is shown in [7, 8] that it can be approximated by a Gaussian random variable with the same variance as $s(n)$ but independent of $s(n)$. The channel is modeled by the complex gain $h_R + jh_I$ and the channel noise is $\nu_R(n) + j\nu_I(n)$. We assume that $\nu_R(n)$ and $\nu_I(n)$ are independent Gaussian noise with variance σ_ν^2. Re$(\cdot)$ denotes taking the real-part of.

3. BLIND EQUALIZATION

Exploring Fig. 1 reveals that ignoring the noise term, the equalizer role is to adjust the phase of the received signal

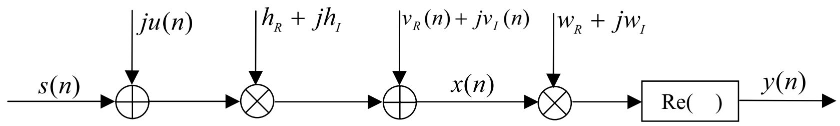

Fig. 1. System Model

such that its real part contains the PAM portion of $x(n)$ only. At the same time, the magnitude response of the equalizer adjusts and recovers PAM symbols to the desired amplitude.

Noting these and following [6], in [7, 8] the following cost function has been defined

$$\xi = E[(|y(n)|^p - R)^2] \quad (1)$$

where $E[\cdot]$ denotes statistical expectation, p is an integer and R is a real-valued constant. A least-mean-square (LMS) type algorithm has also been proposed for adaptation of w_R and w_I. Moreover, the choice of $p = 1$ has been recognized appropriate for this application [7, 8]. In the next section, we present a thorough analysis of the cost function ξ and theoretically confirm the predictions made in [7, 8] through computer simulations. Because of the limited space, here, the analysis is given only for the case of binary symbols where $s(n) = \pm 1$ and $R = 1$.

4. PERFORMANCE SURFACE

For $p = 1$ and binary symbols $s(n)$,

$$\xi = E[(|y(n)| - 1)^2]. \quad (2)$$

From Fig. 1,we obtain the expansion $y(n)$ as

$$\begin{aligned} y(n) &= \begin{bmatrix} s(n) & -u(n) \end{bmatrix} \mathbf{H} \begin{bmatrix} w_R \\ w_I \end{bmatrix} \\ &+ \begin{bmatrix} \nu_R(n) & -\nu_I(n) \end{bmatrix} \begin{bmatrix} w_R \\ w_I \end{bmatrix} \end{aligned} \quad (3)$$

where $\mathbf{H} = \begin{bmatrix} h_R & -h_I \\ h_I & h_R \end{bmatrix}$.

Direct substitution of (3) in (2) leads to a rather complex expression to analyze. This complex analysis, fortunately, can be avoided if we define $\begin{bmatrix} c_R \\ c_I \end{bmatrix} = \mathbf{H} \begin{bmatrix} w_R \\ w_I \end{bmatrix}$ and $\begin{bmatrix} \nu'_R(n) & -\nu'_I(n) \end{bmatrix} = \begin{bmatrix} \nu_R(n) & -\nu_I(n) \end{bmatrix} \mathbf{H}^{-1}$. Substituting these in (3), we obtain

$$y(n) = (s(n) + \nu'_R(n))c_R - (u(n) + \nu'_I(n))c_I. \quad (4)$$

We can now proceed with a less complex analysis of the cost function (2) in terms of the modified tap weights c_R and c_I.

Before we proceed with our analysis, the followings worth noting. The matrix $\mathbf{H}$ satisfies the identity $\mathbf{H}^T\mathbf{H} = (h_R^2 + h_I^2)\mathbf{I}$, where the superscript T denotes transpose and $\mathbf{I}$ is the identity matrix. This implies that transformation by $\mathbf{H}$ rotates the variable axes and scales them with a factor of $\sqrt{h_R^2 + h_I^2}$. It thus does not change the shape of the performance surface associated with the cost function ξ. It only rotates and scales the performance surface. Hence, analyses of ξ in terms of the variables (w_R, w_I) and (c_R, c_I) are equivalent.

Substituting (4) in (2), expanding the results, and noting that $s(n) = \pm 1$ and the random variables $s(n)$, $u(n)$, $\nu'_R(n)$ and $\nu'_I(n)$ are independent of one another,[1] we obtain

$$\xi = (1 + \sigma_{\nu'}^2)c_R^2 + (1 + \sigma_{\nu'}^2)c_I^2 + 1 - 2E[|y(n)|] \quad (5)$$

where the variance of $u(n)$ is 1 and $\sigma_{\nu'}^2 = \sigma_\nu^2/(h_R^2 + h_I^2)$ is the variance of $\nu'_R(n)$ and $\nu'_I(n)$. Assuming that the binary symbols $s(n)$ are equally distributed, we can obtain

$$E[|y(n)|] = 2c_R \int_0^{\frac{c_R}{\sigma}} f(x)dx + 2\sigma f(\frac{c_R}{\sigma}). \quad (6)$$

where $f(x) = \frac{1}{\sqrt{2\pi}} e^{-x^2/2}$ is the probability distribution function (PDF) of a standard normal distribution, and

$$\sigma = \sqrt{\sigma_{\nu'}^2 c_R^2 + (\sigma_{\nu'}^2 + 1)c_I^2}. \quad (7)$$

Substituting (6) and (7) in (5), we obtain

$$\xi = c_R^2 + \sigma^2 + 1 - 4c_R \int_0^{\frac{c_R}{\sigma}} f(x)dx - 4\sigma f(\frac{c_R}{\sigma}). \quad (8)$$

This is the performance function of the blind equalizer with respect to variables c_R and c_I. By direct inspection of (8), one can see that ξ is symmetric with respect to both c_R and c_I axes.

To find the critical (minimum, maximum and saddle) points of the performance surface ξ, we set the derivatives of ξ with respect to c_R and c_I equal to zero. This, after some manipulations, leads to the following equations [9]

$$(\sigma_{\nu'}^2 + 1)c_R - 2\int_0^{\frac{c_R}{\sigma}} f(x)dx - \frac{2\sigma_{\nu'}^2 c_R f(\frac{c_R}{\sigma})}{\sigma} = 0 \quad (9)$$

$$c_I - 2\frac{c_I f(\frac{c_R}{\sigma})}{\sigma} = 0 \quad (10)$$

[1] The independence of $\nu'_R(n)$ and $\nu'_I(n)$ follows from the independence of $\nu_R(n)$ and $\nu_I(n)$ and the orthogonality of $\mathbf{H}$.

By direct substitution and recalling (7), one can confirm that the following pairs are four distinct solutions to (9) and (10):

$$c_I = 0, \quad c_R = \pm \frac{2\int_0^{\frac{1}{\sigma_{\nu'}}} f(x)dx + 2\sigma_{\nu'} f(\frac{1}{\sigma_{\nu'}})}{1+\sigma_{\nu'}^2} \quad (11)$$

$$c_R = 0, \quad c_I = \pm \frac{2}{\sqrt{2\pi(\sigma_{\nu'}^2+1)}}. \quad (12)$$

In [9], it is shown that these are the only possible solutions to (9) and (10).

Next, we study each of the solutions (11)-(12) to find out they are maximum, minimum or saddle points. To this end, we evaluate the second derivatives of ξ with respect to c_R and c_I and obtain that for (11),

$$\frac{\partial^2\xi}{\partial c_R^2} > 0, \ \frac{\partial^2\xi}{\partial c_I^2} > 0, \ \frac{\partial^2\xi}{\partial c_R^2}\frac{\partial^2\xi}{\partial c_I^2} - \left(\frac{\partial^2\xi}{\partial c_R \partial c_I}\right)^2 > 0, \quad (13)$$

and for (12),

$$\frac{\partial^2\xi}{\partial c_R^2} = 0, \ \frac{\partial^2\xi}{\partial c_I^2} > 0, \ \frac{\partial^2\xi}{\partial c_R^2}\frac{\partial^2\xi}{\partial c_I^2} - \left(\frac{\partial^2\xi}{\partial c_R \partial c_I}\right)^2 = 0. \quad (14)$$

The inequalities (13) imply that (11) are minimum points of the performance surface. The inequalities (14), on the other hand, predict that (12) are either saddle or minimum points of the performance surface. In [9], a study of the latter points has been carried out by visualizing the performance surface and predicting that they are saddle points. In the following section, we mathematically prove that the solutions (12) are in fact saddle points of the performance surface.

5. SADDLE POINTS OF THE PERFORMANCE SURFACE

To prove that the solutions (12) are not minima of the performance surface, hence are saddle points, we recall the symmetry of ξ with respect to c_R and c_I, choose one of these solutions, and show that on any circle that is centered at this solution and has an arbitrarily small radius, there exists at least one point for which ξ is smaller than its value at the center of the circle.

We define $c_R = r\cos\theta$ and $c_I = y_0 + r\sin\theta$ with $y_0 = \frac{2}{\sqrt{2\pi(\sigma_{\nu'}^2+1)}}$, and note that $\{c_R, c_I\}$ with $r = 0$ is one the solutions (12). We will show that given any positive number ϵ, there exists a set of $\{\theta_0, r_0\}$ with $r_0 < \epsilon$ so that $\xi|_{r=r_0,\theta=\theta_0} < \xi|_{r=0}$. To this end, we define

$$\begin{aligned} J &= \xi - \xi|_{r=0} \\ &= c_R^2 + \sigma^2 - \sigma_0^2 + 4\sigma_0 f(0) \\ &\quad -4c_R \int_0^{\frac{c_R}{\sigma}} f(x)dx - 4\sigma f(\frac{c_R}{\sigma}). \end{aligned} \quad (15)$$

where $\sigma_0 = \sigma|_{r=0} = y_0\sqrt{(\sigma_{\nu'}^2+1)}$. Choosing θ such that $\sin\theta = -\frac{r}{2y_0}$ and applying it in (7), we obtain, after some straightforward manipulations,

$$\sigma^2 = \sigma_0^2 - c_R^2. \quad (16)$$

Using (16), (15) becomes

$$J = 4\sigma_0 f(0) - 4c_R \int_0^{\frac{c_R}{\sigma}} f(x)dx - 4\sigma f(\frac{c_R}{\sigma}). \quad (17)$$

Applying Taylor series, we obtain, for $0 < \frac{c_R}{\sigma} < 1$, $\int_0^{\frac{c_R}{\sigma}} f(x)dx > f(0)\left(\frac{c_R}{\sigma} - \frac{1}{6}(\frac{c_R}{\sigma})^3 + \frac{1}{40}(\frac{c_R}{\sigma})^5 - \frac{1}{336}(\frac{c_R}{\sigma})^7\right)$ and $f(\frac{c_R}{\sigma}) > f(0)\left(1 - \frac{1}{2}(\frac{c_R}{\sigma})^2 + \frac{1}{8}(\frac{c_R}{\sigma})^4 - \frac{1}{48}(\frac{c_R}{\sigma})^6\right)$. Substituting these in (17), we obtain, for $0 < \frac{c_R}{\sigma} < 1$,

$$\begin{aligned} J &< -4f(0)\left(\sigma - \sigma_0 + \frac{c_R^2}{2\sigma} - \frac{c_R^4}{24\sigma^3} + \frac{c_R^6}{240\sigma^5} - \frac{c_R^8}{336\sigma^7}\right) \\ &< -4f(0)\left(\sigma - \sigma_0 + \frac{c_R^2}{2\sigma} - \frac{c_R^4}{24\sigma^3}\right) \\ &= -\frac{2f(0)}{\sigma}\left(2\sigma^2 - 2\sigma\sigma_0 + c_R^2 - \frac{c_R^4}{12\sigma^2}\right) \\ &= -\frac{f(0)(\sigma_0-\sigma)^2}{6\sigma^3}\left(12\sigma^2 - (\sigma_0+\sigma)^2\right) \\ &< -\frac{f(0)(\sigma_0-\sigma)^2}{6\sigma^3}\left(12\sigma^2 - 4\sigma_0^2\right) \\ &= -\frac{2f(0)(\sigma_0-\sigma)^2}{3\sigma^3}\left(2\sigma^2 - c_R^2\right). \end{aligned} \quad (18)$$

where the fourth line follows from (16) and the fifth line follows from $\sigma_0 > \sigma$ which is implied by (16). This shows that $J < 0$ when $c_R^2 < 2\sigma^2$. To complete our proof, next we show that this condition can always be satisfied when r is arbitrarily small.

Considering the assumptions we made in above derivations, we summarize the sufficient conditions for $J < 0$ to be $\{\sin\theta = -\frac{r}{2y_0}, 0 < \frac{c_R}{\sigma} < 1\}$. For small values of r, one can always find a real angle θ that satisfies the condition $\sin\theta = -\frac{r}{2y_0}$ since $y_0 = \frac{2}{\sqrt{2\pi(\sigma_{\nu'}^2+1)}}$ is non-zero. On the other hand, the condition $\frac{c_R}{\sigma} < 1$ implies $c_R^2 < \sigma^2$, which is satisfied for small r, since $c_R = r\cos\theta$ and from (16) we observe that $\sigma^2 \approx \sigma_0^2 = y_0^2(\sigma_{\nu'}^2+1)$. This in turn implies that for the selected θ, $c_R^2 < 2\sigma^2$ is always true, and thus $J < 0$.

Fig. 2 presents an example of the performance surface ξ, for the case where $\sigma_{\nu'} = 0.01$. This figure clearly shows that the performance surface ξ has two global minima (corresponding to (11)) and two saddle points (corresponding to (12)).

6. INITIALIZATION STRATEGY

We note that in an actual blind equalizer, it is the tap weights w_R and w_I that should be adapted. Hence the performance

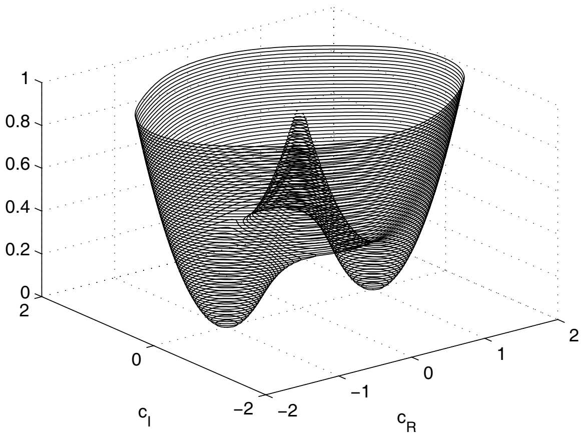

Fig. 2. An example of the performance surface.

surface is a rotated and scaled version of that shown in Fig. 2. Of course the amount of rotation and scaling factor are unknown. Hence, an arbitrary initialization of w_R and w_I may coincide with a point on the performance surface that can be trapped for some iterations near one of the saddle points, and eventually converges to one of the global minima. If we choose an initial point $\{w_R, w_I\}$ near origin, after rotating and scaling, $\{c_R, c_I\}$ should be also near origin, which will converge to one of the global minima quickly. Fig. 3 presents four trajectories showing the convergence of the blind LMS algorithm. The trajectories are time scaled by stars which show convergence after every 50 iterations. As seen, the two points that start from near the origin converge to the global minima after about 100 iterations. On the other hand, one of the points that is initialized to a point right below a saddle point of the surface is trapped for many iterations near this saddle point before finding its way towards one of the global minima.

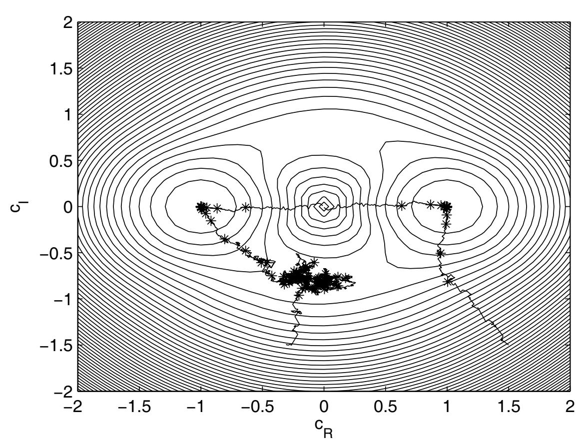

Fig. 3. Examples of trajectories of the blind LMS algorithm.

7. CONCLUSION

A thorough analysis of a recently proposed blind equalizer [7, 8] was presented. A mathematical expression of the performance surface that characterizes this blind equalizer was developed and a limited analysis of it was presented in [9]. In this paper, we completed the latter study and proved that the performance surface of the blind equalizer is characterized by two minimum and two saddle points.

8. REFERENCES

[1] J.G. Proakis, *Digital Communications*, 3rd Edition, New York: McGraw Hill, 1995.

[2] T. Starr, J.M. Cioffi, and P.J. Silverman, *Understanding Digital Subscriber Line Technology*, Prentice Hall, 1999.

[3] R. Van Nee, and R. Prasad, *OFDM for Wireless Multimedia Communications.* Arthec House, 2000.

[4] S.D. Sandberg and M.A. Tzannes, "Overlapped Discrete Multitone Modulation for High Speed Copper Wire Communications," *IEEE JSAC*, vol. 13, no. 9, pp. 1571-1585, Dec. 1995.

[5] P.P. Vaidyanathan, *Multirate Systems and Filter Banks.* Englewood Cliffs, New Jersey, Prentice Hall, 1993.

[6] D. N. Godard, "Self-recovering equalization and carrier tracking in a two-dimensional data communication system," *IEEE Trans. Commun.,* vol. COM-28, pp. 1867-1875, Sept. 1980.

[7] B. Farhang-Boroujeny, "Multicarrier modulation with blind detection capability using cosine modulated filterbanks," *IEEE Trans. Commun.,* vol. 51, no. 12, pp. 2057-2070, Dec. 2003.

[8] B. Farhang-Boroujeny, "Discrete multitone modulation with blind detection capability," in Proceedings of Vehicular Technology Conference, vol. 1, pp. 376-380, Sept. 2002.

[9] L. Lin, B. Farhang-Boroujeny, "Convergence Analysis of Blind Equalizer in a Cosine Modulated Filter Bank - Based Multicarrier Communication System," in Proceedings of IEEE Workshop on Signal Processing Advances in Wireless Communications, pp. 368-372, June 2003.